IL NUOVO CIMENTO Vol. 30 C, N. 5 Settembre-Ottobre 2007
DOI 10.1393/ncc/i2008-10259-7

The MEMS project(*)

R. Battiston
Dipartimento di Fisica and INFN, Sezione di Perugia - Perugia, Italy

(ricevuto il 3 Marzo 2008; pubblicato online il 23 Aprile 2008)

Summary. — We report on the results of the first three years of the INFN/FBK-irst "MEMS Project", a program aiming to develop innovative silicon-based radiation detectors using MEMS-like technologies.

PACS 29.40.-n – Radiation detectors.
PACS 29.40.Gx – Tracking and position-sensitive detectors.
PACS 29.40.Wk – Solid-state detectors.

1. – Introduction

The potential for new discoveries is often linked to the availability of new measurement techniques. In the field of particle physics, a relevant example is the development, started in the 70s, of silicon detectors based on the CMOS technology derived from the microelectronics applications. It has been instrumental for the development of modern tracking detectors and imaging calorimeters used both at accelerators as well in space experiments. The technologies at the basis of the Micro Electronic Mechanical Systems (MEMS) open the possibility of developing completely new detectors for particle and fundamental physics, exploiting not only the electrical properties of silicon, but also its mechanical and thermal characteristics. In order to explore further the potential of MEMS application for particle physics, in 2004, INFN and the Provincia Autonoma di Trento (PAT), have agreed to a collaborative effort, the MEMS research project, which is finalized to the development of new radiation detectors. The MEMS project is driven by a "dual goal": on one side, to respond to the requirement of frontier research in the field of particle and fundamental physics, on the other side to identify consumer applications for these technologies.

During the last 10 years INFN and ITC-irst (now FBK-irst), the main PAT research Institute, have collaborated on a number of projects, both for ground-based and space-based research applications: the success of this collaboration is based on the fact that

(*) Paper presented at the 1st Workshop on Photon Detection for High Energy Medical and Space Applications; Perugia, June 13-14, 2007.

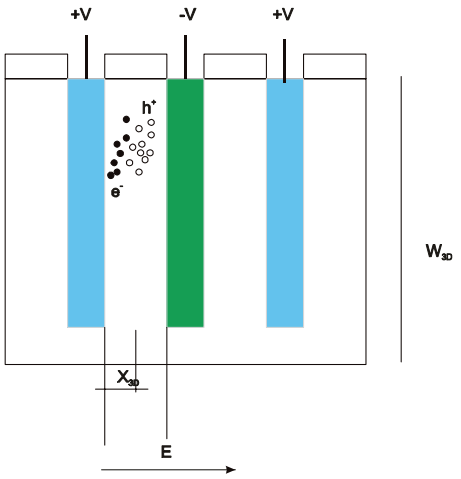

Fig. 1. – Schematic view of a 3D detector.

each Institute contributes with competences which are complementary. On one side INFN is very active in identifying demanding research applications, in the context of international collaborations. On the other side the FBK-irst laboratory has reached a level of organization and production quality, which is close to industry. In addition, one of the goals of the FBK-irst is to bridge the gap between the research and applications, a gap, which in Italy is particularly significant. For this reason the MEMS project could become an example of good practice in the field of technology transfer in Italy, providing "turn key" new products for the industry, which are motivated from frontier research innovations.

Since the fall of 2003, the start of the project, we have identified four pilot projects, which have been chosen because of their potential in revolutionizing four corresponding research fields:

- Three-dimensional silicon detectors (3DSi).
- Solid-state single-photon detectors, also called Silicon PhotoMultipliers (SiPM).
- Array of cryogenic bolometers for measuring the CMB.
- Cryogenic, thick silicon for the search of rare events.

These projects have been developed in collaboration with Italian INFN groups, active in the field of radiation detectors developments also through the support of the Vth INFN Committee. In the following we review the main results obtained on the pilot MEMS projects during the first two and half years of the program.

2. – 3D silicon radiation detectors

2˙1. *Introduction.* – Planar silicon detectors collect the charge on the wafers surfaces: the generation volume, the electric field intensity and the path traveled by the charges, all depend on the wafer thickness. Tri-dimensional (3D) silicon detectors are based on electrodes running perpendicular to the wafer surface, partly or fully across its thickness (fig. 1).

In this way, the generation volume is still determined by the detector thickness, but the drift volume and the interelectrode distance determine the electric field. Since this distance can be reduced to few tens of micron, these detectors can be operated at a much lower depletion voltage, while the charge collection is much faster than in the case of traditional detectors. This geometry also assures full charge collection and lower intrinsic noise. The development of these detectors, started by S. Parker *et al.* at the end of the 90s, requires MEMS technologies, in particular the Deep-Reactive Ion Etching (DRIE). The fabrication of 3D detectors is based on laser drilling of holes, while the electrodes are realized by Schottky contacts using metal deposition. Thanks to their electrode geometry, 3D detectors are intrinsically radiation resistant. For this reason they are a good candidate for replacing pixel detectors on Inner Tracking Systems. Due to the lack of edge effects and their intrinsic speed, they also find interesting applications in the field of medical or industrial X-ray imaging, as well on DNA sequencing using radioactive tracers.

2˙2. *Development at FBK-irst.* – For the MEMS project, we have produced three lots of $\sim 1.6\,\mathrm{k\Omega cm}$, *p*-type, $\langle 111\rangle$, $380\,\mu$m wafers, using 3D STC (Single Type Column) fabrication technology, with $180\,\mu$m deep DRIE holes (fabricated at CNM, Barcellona, Spain and IBS, Peynier, France). Surface insulation is obtained by a combination of *p*-stop and *p*-spray [1-3]. *I-V* characteristics show an average columnar density $< 1\,\mathrm{pA}$ with a detector yield of about 90%. The first two batches have been irradiated using the TRIGA facility of the Jozef Stefan Laboratory in Lubiana, Slovenia, at the following 6 fluences, which were followed by a 15 days, ambient temperature annealing:

$$F_1 = 5\times10^{13}\,\mathrm{n/cm^2}; \qquad F_2 = 1\times10^{14}\,\mathrm{n/cm^2},$$
$$F_3 = 2\times10^{14}\,\mathrm{n/cm^2}; \qquad F_4 = 5\times10^{14}\,\mathrm{n/cm^2},$$
$$F_5 = 1\times10^{15}\,\mathrm{n/cm^2}; \qquad F_6 = 5\times10^{15}\,\mathrm{n/cm^2}.$$

The electrical tests (*I-V* and *C-V*) were performed in darkness, at 23 °C. From the analysis of the data, we observe that the depletion voltages, V_{depl}, as a function of the dose are in agreement with the expectations (fig. 2). These 3D detectors are completely depleted below 1000 V even with fluences of $1\times10^{16}\,\mathrm{n/cm^2}$, while a planar detector would require one order of magnitude higher V_{depl}.

Charge Collection Efficiency (CCE) has been measured using a 90 Sr β source. β particles are collimated on the detector, which is then polarized up to 400 V; a trigger is provided by a scintillating tile read by a photomultiplier. Current signals are amplified by an Amptek circuit, with a $2.4\,\mu$s shaping time and a noise figure of 1500 e- r.m.s. Already at 0 V we observe a CCE of 27%, an effect characteristic of the 3D geometry. At 190 V we obtain 100% CCE. In fig. 3 we show the charge collected as a function of the depletion voltage and the good S/N separation: these data correspond to a 3D diode on a $500\,\mu$m thick FZ substrate, with a column pitch of $100\,\mu$m.

The next technological step will include the implementation of two types of alternated *n* and *p* column (*Double Type Column*, DTC, technology), starting from the opposite side of the wafer and stopping at $50\,\mu$m from the surface (fig. 4).

The development of FBK-Irst 3D detectors is attracting the interest of high-energy physics groups like:

– ATLAS, for the *up-grading* of the b-*layer* of the tracking detector,

– CMS, for the inner tracking upgrade,

– P326, for the development of the GIGATRACKER detector.

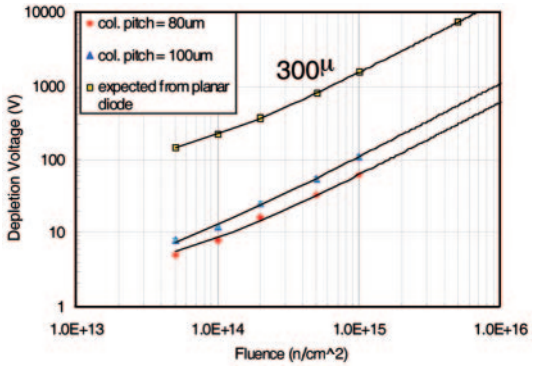

Fig. 2. – Depletion voltages *vs.* fluence for two kinds of 3D diodes. The equivalent values for a planar 300 μm diode are also shown.

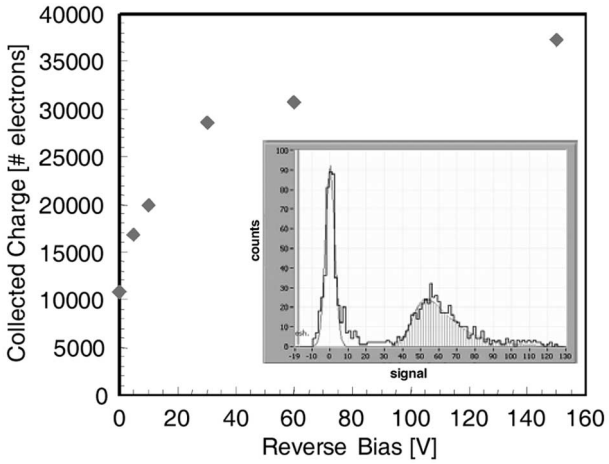

Fig. 3. – Collected charge *vs.* depletion voltage for a 500 μm thick 3D diode. In the small square the good signal *vs.* noise separation at 5 V is also shown.

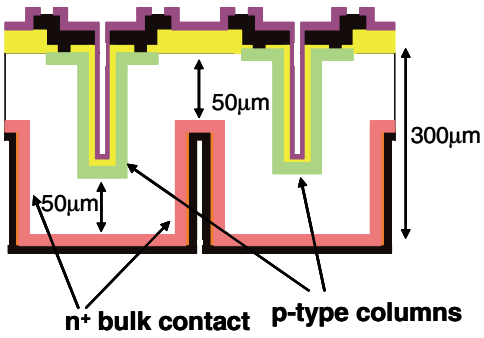

Fig. 4. – Layout of a 3D-dtc detector with alternating columns.

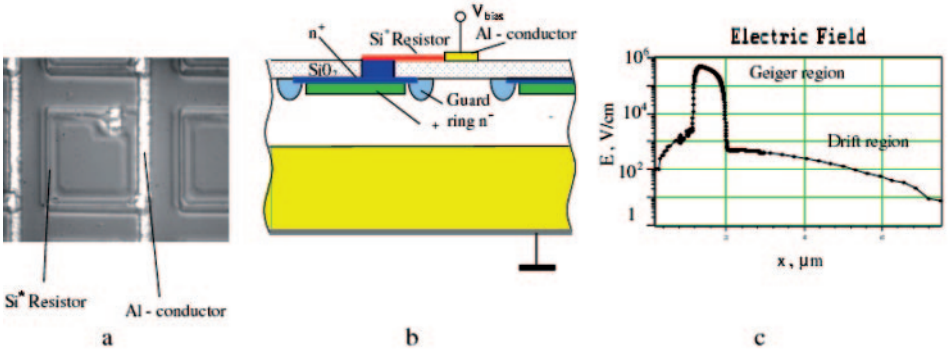

Fig. 5. – (a) SEM microphotography of a SiPM micropixel, (b) schematic section of the micropixel, (c) electric field dependence through a vertical section of the micropixel.

For more information on the 3D detectors at FBK-Irst, you are invited to look at the web page `http://tredi.itc.it/`.

3. – Silicon photomultipliers, SiPM

3˙1. *Introduction.* – Silicon Photomultipliers (SiPM) are arrays of semiconductor photon detectors (micropixel) operating in Geiger mode [4]. The micropixels, having typical sizes of tens of microns, are built on a common substrate; all of them are interconnected through an integrated, decoupling resistor R to a common polarization strip (fig. 5).

The polarization voltage is chosen 10–20% above the breakdown voltage, ensuring a high probability for a free charge to start a Geiger discharge. The discharge is self-quenched when the voltage goes below the breakdown voltage, due to the voltage drop across the resistor R. Each micropixel behaves like a binary counter for single photons. The array provides an output signal, which is the analog sum of the digital micropixel signals, measuring the intensity of the incoming radiation. From the technological point of view (fig. 5b), the fabrication of the SiPM is based on wafers having an epitaxial layer. The thickness of this layer (few micron) and the wafer resistivity are chosen to ensure a good QE for the wavelength of interest and a quick charge collection. The heart of the device is the inversely polarized $n+/p$ junction. The additional p region contributes to control the discharge phenomenon, limiting its development within the planar junction volume. The junction depth is limited to the minimum needed for a good QE (fig. 5c). In order to limit the operation voltage to a few tens of Volts, the doping level of the additional p layer has to be carefully chosen. In order to limit breakdown phenomena at the junction edge, an n-guard ring is added, to improve the decoupling among nearby micropixels. The size of the guard ring is critical, since it influences the geometrical efficiency of the device. The integrated resistor is made of polysilicon, a widely used technology at FBK-irst.

The performances of SiPM are very interesting, in particular if compared to other kinds of photomultipliers (see table I): high gain ($\sim 10^6$) with low operating voltages ($\sim 30\,\mathrm{V}$), operational stability, insensibility to the magnetic field, excellent time resolution ($< 30\,\mathrm{ps}$), single-photon detection, possibility to operate at room temperature although best noise performances are obtained at lower temperatures (up to $-70\,^\circ\mathrm{C}$). The SiPM dynamic range is directly proportional to the number of micropixel in the array; for this reason it is important to build very small but highly efficient, micropixels.

TABLE I. – *Comparison of SiPM produced at FBK-irst with other solid-state photomultipliers.*

	PMT	APD	HPD	SiPM
Photon detection efficiency:				(geom. eff. 0.5)
Blue (450 nm)	20%	50%	20%	30%
Green–Yellow (550 nm)	a few%	60÷70%	a few%	35%
Red (650 nm)	$< 1\%$	80%	$< 1\%$	30%
Gain	10^6–10^7	100–200	10^3	10^6
Operation voltage	1–2 kV	100–500 V	20 kV	25 V
Operation in the magnetic field	problematic	OK	OK	OK
Threshold sensitivity ($S/N \gg 1$)	1 ph.e.	$\sim$ 10 ph.e.	1 ph.e.	1 ph.e.
Timing /10 ph.e.	$\sim$ 100 ps	a few ns	$\sim$ 100 ps	30 ps
Dynamic range	$\sim 10^6$	large	large	$\sim 10^3/\,\mathrm{mm}^2$
Complexity	High: vacuum, high voltage	Medium: low-noise electronics	very high: hybrid technology, very high voltage	relatively low

Currently, the limiting factor for the SiPM in the single-photon detection mode is the noise rate due to the dark current, typically few MHz/mm^2 (at 300 K) or 1 kHz/mm^2 (at 100 K). Due to the random properties of the noise signals, increasing the threshold of the output signal to value corresponding to two (or more) simultaneous pulses reduces the noise rates by order(s) of magnitude.

For these reasons the SiPM is quickly becoming a very interesting device for all applications where the detection of very low optical signals is required. Among the many applications we recall the detection of single UV photons, the detection of signal from scintillating fibers in trackers of calorimeters both in high-energy physics as well as in medical imaging and optical telecommunications.

3˙2. *Development at FBK-irst.* – Three batches of SiPM have been developed at FBK-irst within the MEMS program [5,6]. The first and the second were devoted to develop the technology, checking the performances reported in the literature. The study of the noise and the cross talk among micropixels were among the goals of these production batches. The process requires 10 photolithography masks, with micron size features. The third batch is the first production batch with geometries optimized for specific applications.

The detailed characterization of the first two technology batches has provided important information on the devices produced at FBK-irst, allowing a detailed comparison with devices of the same type produced elsewhere.

Signal and noise characteristics

The devices produces three kinds of signals: i) single pulses due to a single micro cell activation, ii) double (triple) amplitude pulses due to the simultaneous activation of few micro cells (expected for instance in case of optical cross-talk and iii) pulse of

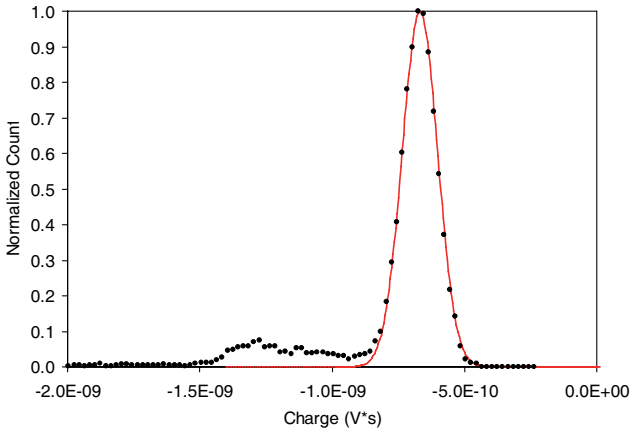

Fig. 6. – FBK-irst SiPM charge spectrum (integration time 100 ns).

smaller amplitudes, following a normal (large) pulse (typical of after-pulses). Integrating the signals over 100 ns, in order to fully include the width of single pulses, we obtain the spectrum shown in fig. 6. The large peak, dominating the spectrum, corresponds to single "monochromatic" pulses and shows the good performance of the detector; the tail corresponds to events with larger charge deposition due to optical cross-talk and/or after pulses.

The gain (corresponding to the peak position) grows linearly with the polarization voltage, reaching about 10^6 at about 3 V above the breakdown. The measured dark count is of the order of one MHz at the breakdown voltage (32 V), and reaches 2–3 MHz at 3 V over-voltage. The width of the stability plateau is about 4–5 V.

Photodetection efficiency

In order to measure the SiPM Photo Detection Efficiency (PDE) we have done two kinds of measurements. After illuminating the device with a suitable light source we have measured the DC value of the current: the difference between the measured value and the dark current is proportional to the number of detected photons, through the gain, which has to be known. The second method consists in the measurement of the counting rate: the difference between the measured rate and the dark rate measures the number of detected photons. The two methods give a good agreement: the result obtained for a device having a 20% active area is shown in fig. 7.

The figure shows the PDE as a function of the light wavelength and for different polarization voltages. In order to understand the shape of the curves it is necessary to analyze the factors influencing the PDE: the geometrical efficiency (A_e), the quantum efficiency (QE) and the avalanche probability (P_t). A_e is independent of the polarization voltage as well of the wavelength and determines the maximum value that the PDE can reach (0.2 in this case). P_t depends both on the polarization voltage (the ionization yield increases with the voltage) as well as on the wavelength (different absorption depth at different wavelengths). QE depends on the wavelength since both the transmittance of the antireflective coating and the internal quantum efficiency depend on the wavelength.

The PDE dependence on the voltage is due only to P_t, while the wavelength dependence depends both on P_t as well as QE. QE has been measured on diodes from the same wafers, as is shown in fig. 8.

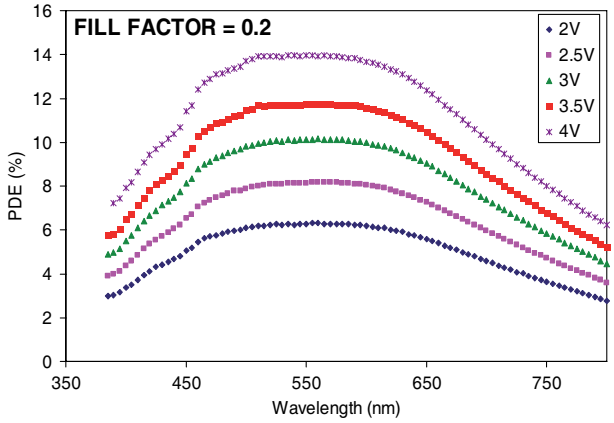

Fig. 7. – FBK-irst Photo Detection Efficiency (PDE) as a function of wavelength.

We can see that the QE is close to 100% for a wavelength of 420 nm, while quickly drops below 400 nm. From this result, we understand that the PDE dependence around 400 nm is limited by Pt. For wavelengths greater than 600 nm the QE is the limiting factor.

Timing resolution

The measurement of the timing characteristics of the SiPM has been done in collaboration with CNR Pisa, using a laser which can provide 60 fs pulses at a rate of 80 MHz with a jitter lower than 100 fs between pulses [7].

The results of the analysis of the time structure of the measured pulses are shown in fig. 9 as a function of the breakdown voltage. An excellent single-photon time resolution of 70 ps has been measured at 3–4 V above breakdown; the time resolution has been observed to improve with $N^{-1/2}$, where N is the number of incident photons.

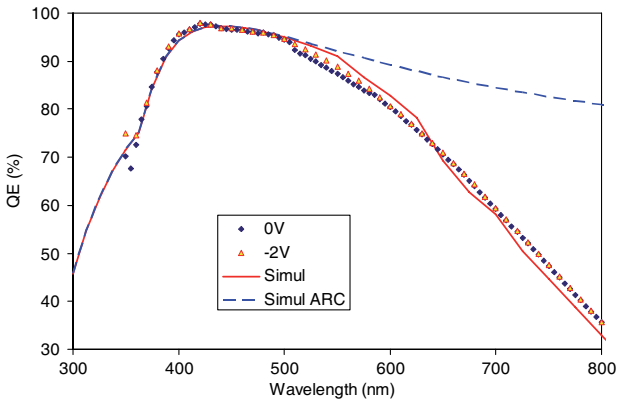

Fig. 8. – Quantum Efficiency (QE) as a function of the wavelength for a diode built with the same technology as the SiPM.

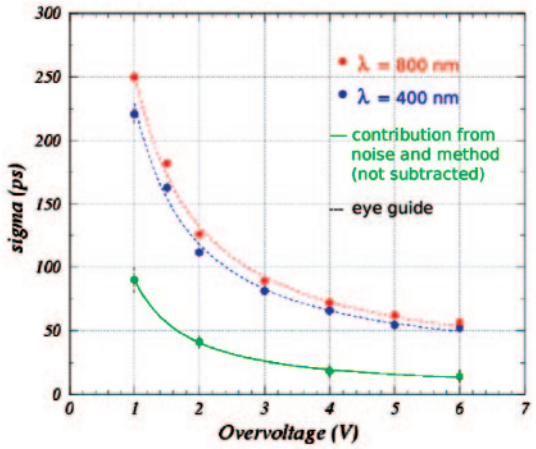

Fig. 9. – SiPM timing resolution as a function of the polarization voltage (referred to the breakdown voltage).

Energy resolution

The good PDE will allow the use of SiPM for the measurement of energy deposition in scintillating media. The energy resolution of a SiPM detector has been measured irradiating with a ^{22}Na source a LSO crystal of $1 \times 1 \times 10\,\mathrm{mm}^3$. We observed energy resolution of 21% FWHM, suitable for PET applications [8].

In 2007 we have produced a third batch, using the technology derived from the first runs and implementing various geometries suitable for applications which ranges from PET, fiber tracking, calorimetry, Cerenkov light detections and so on. In particular the first arrays of SiPM have been produced, with up to 32 channels each (fig. 10).

The yield observed on this first large production run exceeds 90%, with several thousand SiPM produced, and the properties measured are very uniform among different devices from the same wafer. Applications of the FBK-irst SiPM for scientific applications are steadily increasing, as has been presented at this conference.

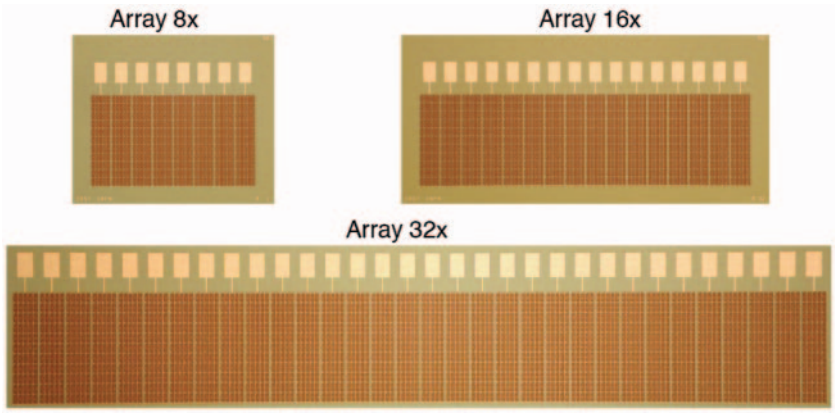

Fig. 10. – SiPM arrays produced at FBK-irst in 2007 (third batch).

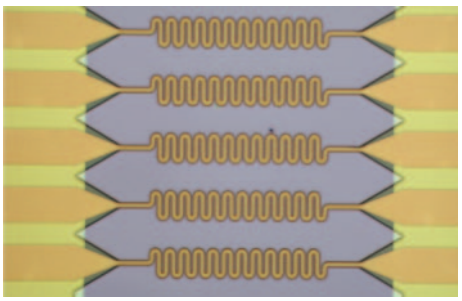

Fig. 11. – CFL2 microwires on Ti. Metal film thickness 200 nm, strip width 20 microns, strip length 6 mm, edge-to-edge distance 2 mm. The mechanical structure is reinforced by a polyamide layer (4 micron of thickness).

4. – Development of arrays of cryogenic microbolometers

4˙1. *Introduction.* – Bolometers are a versatile kind of radiation sensor used for long time in various fields of physics and astrophysics as well as in industrial applications, like medical and environmental. Cryogenic bolometers have been used for years in the search of rare nuclear decays, and FBK-irst has a solid experience in the development of this kind of sensors in collaboration with the INFN group of Milan working on double beta-decay and neutrino mass determination.

Typically two kinds of technologies are used: the first makes use of diffuse resistors, doped to the Mott limit, as thermal sensors coupled to silicon elements, the second one is based on the properties of superconducting materials close to the transition temperature, coupled to dielectric materials.

While FBK-irst has an established knowledge on the first technology, an example of suspended micro wires in shown in fig. 11, within the MEMS project we started the development of the second technology, aiming at the development of bolometers arrays for the imaging of the CMB radiation and of its polarization. A promising technology is the so-called *Kinetic Inductance Detectors* (KID), superconducting devices sensitive to the deposition of RF radiation, which changes their electrical properties. If KIDs are used as elements of an array of resonant circuits, the intensity of RF radiation is determined by the variation of the resonators properties.

Fig. 12. – Microwave resonators coupled to a CPW line.

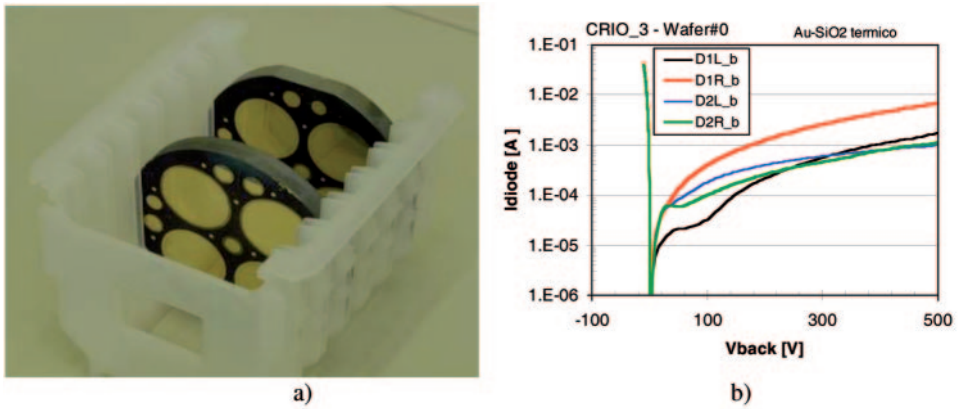

Fig. 13. – a) 1 cm thick n wafers with Au/Si Shottky barrier; b) I-V characteristics at room temperature of the four large-area diodes.

4˙2. *Development at FBK-irst.* – After some initial tests of structures niobium-based superconducting devices, which have shown problems in the purity of the evaporated Nb layer, we have concentrated our efforts on Al resonators deposited by sputtering. Various geometries have been built to study the influence of the substrate on the phase noise. One interesting structure is shown in fig. 12, where the conductor and the surrounding ground plane are separated by a 4 micron deep trench. These devices have been sent to the AIF laboratory in Cardiff for the first cryogenic tests at low temperature. Al strips have a lower superconductive transition temperature than Nb, around 1.2 K; they should then be tested in the 100 mK range.

5. – Cryogenic silicon time projection chamber

5˙1. *Introduction.* – Silicon detectors for radiation detectors are traditionally based on doped semiconductors operating at ambient temperature. This technology limits the active volume of the detectors (depletion layer) to few mm with fairly large depletion voltages. In various applications one would need much larger active volumes: this can be obtained operating at cryogenic temperatures. At the "freeze-out" temperature the depletion is complete even for intrinsic silicon as there is no need to apply large voltages to remove the carriers generated inside the bulk. In this way it is also easier to model the electric fields in the bulk and to design focusing and amplification structures. At low temperature the electrons mean free path in silicon is 5–10 micron, much larger than at room temperature. The development of large volume detectors, in the range of 1 kg of mass, would open application windows on fields like solar neutrino physics, coherent neutrino scattering, dark matter search, fast neutron detectors and so on. Preliminary results on the properties of thick silicon have been reported in the past, showing promising performances. For instance a 1 cm thick diode operating at 90 K at LNL has shown very low dark current, in the range of tens of fA at 100 V of bias, detecting X- and gamma-particles.

5˙2. *Development at FBK-irst.* – The goal of the development at FBK-irst was to develop for the first time large semiconductor active volumes, making use of the milliseconds electrons lifetime of high-resistivity silicon (20 kΩcm) operated at cryogenic temperatures with meter long attenuation lengths. A Schottky junction has been developed, after trying different kinds of metals for the barrier, concentrating on Au/Si

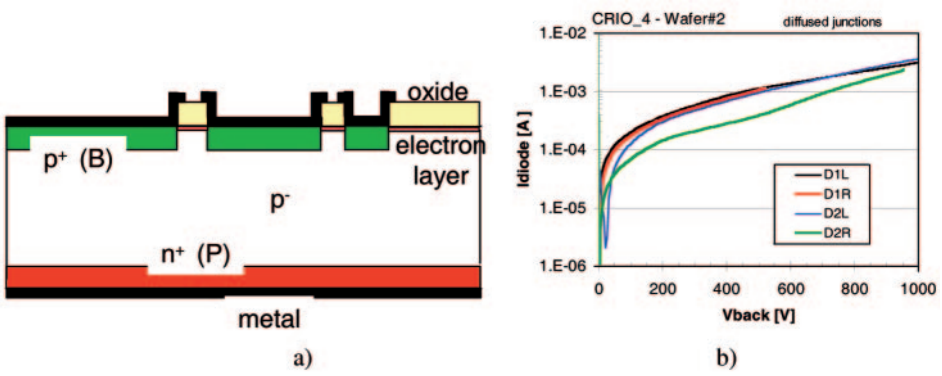

Fig. 14. – a) Scheme of the p diodes built using a diffusion doping process. The upper side (diode with guard rings) is doped using B. b) I-V characteristics at room temperature of the four large-area p diodes.

junctions. We then tried FZ wafers having resisitivities higher than 30 kΩcm and thickness of 1.5 mm. We tried both n and p wafers. After measuring the basic parameters on these wafers, construction of 1 cm thick wafers started; manipulating these large wafers has required modifications to the fab-line processes and solving various technical problems. Figure 13a shows the photograph of two 1 cm thick wafers, built with the Au/Si barrier technology. Figure 13b show the I-V characteristics of n-type substrates at ambient temperature. The rectifying diode properties and the capability of these devices to stand high reverse voltages are clearly visible.

During 2006 we tested B and P diffusion-doped pn junctions on 1 cm thick wafers following the scheme of fig. 14a which is viable for p substrates operating at cryogenic temperatures due to the *freeze-out* of the carriers. Figure 14b shows the I-V characteristics for the 4 large diodes on a 1 cm thick wafer; just a few volts are sufficient to substantially deplete the device.

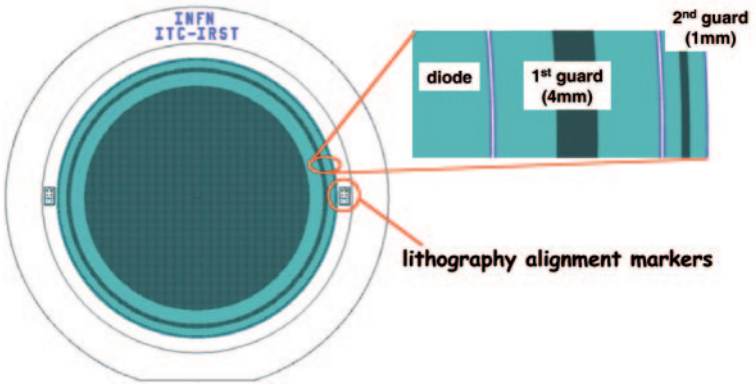

Fig. 15. – Wafer layout showing a single circular diode with diameter of 6.28 cm (area 31 cm^2). The enlarged view shows the details of the guard ring area.

We then built 1 cm thick n-type high-resistivity wafers, purchasing a n-type ingot with resistivity $> 30\,\mathrm{k}\Omega\mathrm{cm}$: from this ingot we cut 12 wafers. The layout is shown in fig. 15. The sensors were characterized cryogenically at LNL, using both gamma sources and cosmic rays. At liquid He temperatures we measured dark currents are at the level of $1\,\mathrm{pA/cm^2}$ or less. Capacitance measurements confirmed the complete depletion due to the "freeze-out" effect. The measured charge collection efficiency shows that with an n-type substrate full efficiency starts already at 100 V. p-type substrates, having higher resistivity, show the same behavior already from 70 V. Using these devices we have measured 4.2 keV (FWHM) of resolution for a 59 keV gamma-ray produced by an Am source. These results are very encouraging, and we are now developing improved charge collection/amplification structures as well as drift structures.

* * *

The MEMS project is based on the collaborative effort of a large number of researchers both from FBK-irst as well as from INFN. The author would like to particularly thank: G. Ambrosi, B. Angelini, P. Bellutti, M. Boscardin, L. Bosisio, U. Bottigli, G. Bressi, G. Carugno, G. Collazuol, P. dal Piaz, P. de Bernardis, A. del Guerra, N. Dinu, S. Haino, M. Ionica, G. Llosa, S. Marcatili, B. Margesin, A. Monfardini, M. Petasecca, A. Papi, C. Piemonte, M. Zen and N. Zorzi.

REFERENCES

[1] Pozza A., Boscardin M., Piemonte C., Dalla Betta G.-F., Bosisio L., Ronchin S. and Zorzi N., *Nucl. Instrum. Methods A*, **570** (2007) 317.
[2] Boscardin M., Bosisio L., Dalla Betta G. F., Piemonte C., Pozza A., Ronchin S., Tosi C. and Zorzi N., *Nucl. Instrum. Methods A*, **572** (2007) 284.
[3] Ronchin S., Boscardin M., Piemonte C., Pozza A., Zorzi N., Dalla Betta G. F., Pellegrini G. and Bosisio L., *Nucl. Instrum. Methods A*, **573** (2007) 224.
[4] Bondarenko G. *et al.*, *Nucl. Instrum. Methods A*, **242** (2000) 187.
[5] Piemonte C., *Nucl. Instrum. Methods A*, **568** (2006) 224.
[6] Piemonte C., Battiston R., Boscardin M., Dalla Betta G.-F., Del Guerra A., Dinu N., Pozza A. and Zorzi N., *IEEE Trans. Nucl. Sci.*, **54** (2007) 236.
[7] Collazuol G., Ambrosi G., Boscardin M., Corsi F., Dalla Betta G. F., Del Guerra A., Galimberti M., Giulietti D., Gizzi L. A., Labate L., Llosa G., Marcatili S., Piemonte C., Pozza A. and Zorzi N., presented at the *XI VCI, Vienna 19-24 February 2007*, to be published in *Nucl. Instrum. Methods A*.
[8] Llosa G., Belcari N., Collazuol G., Del Guerra A., Marcatili S., Moehrs S. and Piemonte C., 2007 *IEEE Nuclear Science Symposium and Medical Imaging Conference, Honolulu, USA, October 28-November 3, 2007*, in press.